Load Change Case Study of an Islanded Photovoltaic-Battery Unit Controlled by Grid-Forming Droop

Luana C. S. Soares * **Pedro A. de Alcântara** *
Lindemberg R. de Lima ** **Camila M. V. Barros** ***
Luciano S. Barros *** **André C. do Nascimento** ****

* *Electrical Engineering Graduate Program, Federal University of Paraiba, PB (e-mails: luana.soares@cear.ufpb.br, pedro.alcantra@cear.ufpb.br)*
** *Mathematics and Computational Modeling Graduate Program, Federal University of Paraiba, PB (e-mail: lindemberg.roberto@academico.ufpb.br)*
*** *Computer System Department, Federal University of Paraiba, PB (e-mails: camila.barros@ci.ufpb.br, lsalesbarros@ci.ufpb.br)*
**** *Department of Education, Control and Industrial Processes, Federal Institute of Pará, PA (e-mail: andre.nascimento@ifpa.edu.br)*

Abstract: Photovoltaic generation does not have the capacity to compensate imbalances between generation and load demand, which can occur in islanded operation of microgrids and cause voltage and frequency deviations. Thus, battery energy storage systems are inserted to support microgrid regulation, what constitutes the hybrid generation units. In these units, grid interface inverter is driven through a grid-forming droop control, as long as photovoltaic and battery DC-DC converters are controlled to promote power balance between generation and load demand. When there is only one hybrid unit in the microgrid, battery charging limit and maximum state-of-charge must also be taken into consideration since supplying of imbalances cannot be shared; and if battery experiences one of these conditions, photovoltaic curtailment is conducted. This paper proposes to test a hybrid unit supplying variable load in islanded mode to evaluate the effectiveness of the grid forming droop control. Through accurate simulations, efficacy of this control strategy is validated for different load, PV generation, and battery conditions.

Keywords: battery charging limit; battery state-of-charge; grid-forming droop control; hybrid photovoltaic/battery-based source; islanded microgrid; PV power curtailment.

1. INTRODUCTION

Microgrids are self-sufficient energy systems that can combine dispersed loads, energy storage systems (ESS), and distributed energy resources (DER) into a controllable system that delivers electricity dependably, flexibly, and intelligently. Microgrids have grown increasingly appealing and might offer a solution for energy redevelopment as a result of the growing penetration of distributed generators, particularly photovoltaic (PV) generations (Guerrero et al., 2013). Additionally, microgrids can be built up in a single-phase, three-phase, or hybrid single/three-phase design depending on the demand and generation requirements. They can also operate in grid-connected or islanded modes (Karimi et al., 2017b).

Microgrids do not have the full capacity to make up for imbalances between generation and load demand in their islanded operation since DERs are mostly intermittent. Therefore, an ESS is necessary for these applications (Mahmood et al., 2015; Mahmood and Jiang, 2019). Despite the availability of numerous ESSs, battery banks have mostly been utilized in practical applications due to cost (de Matos et al., 2015). These systems work well and react rapidly, which helps them to regulate the grid's frequency and voltage. In Fig. 1, a battery energy storage system (BESS) and PV are connected forming a hybrid source configuration. BESSs can also be connected separately, but the hybrid configuration has the advantage of being more economical (Karimi et al., 2017b).

The microgrid control system must operate correctly in islanded mode to manage power efficiently while taking into consideration load-rated power, PV generation, and state-of-charge (SoC) of the batteries (Karimi et al., 2017a). To function in this mode, the controller must regulate voltage and frequency, maintain generation and load demand balance, and safeguard the batteries from deep draining or overcharging (Golsorkhi et al., 2017). A grid-forming strategy is adopted to actively control unit power output, making it possible to support the system voltage and frequency (Karimi et al., 2017b; Pattabiraman et al., 2018). In Karimi et al. (2017a,b), a grid-forming decentralized method for load sharing and power management in a hybrid microgrid is seen that takes into account the available PV power and battery conditions of the units

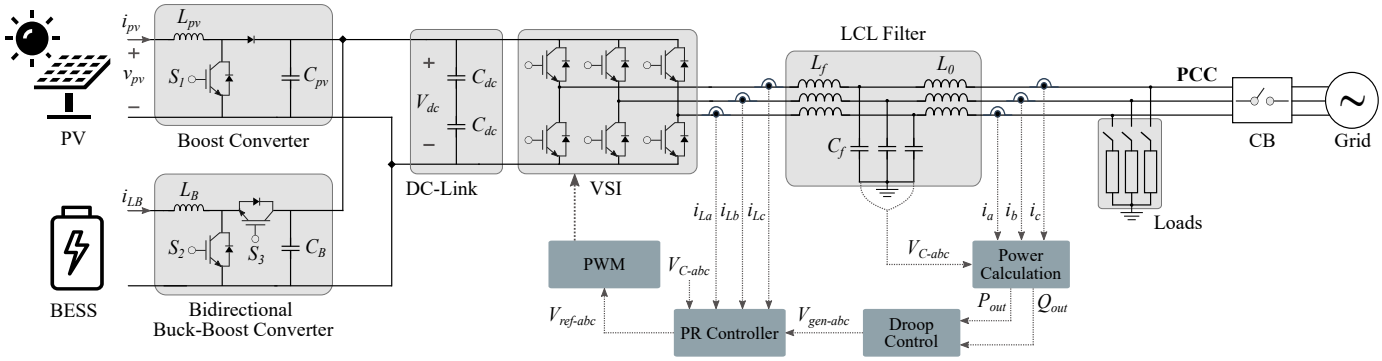

Figure 1. Three-phase microgrid architecture with one hybrid source unit.

to share the load among them. In Mahmood et al. (2012), a control strategy for a standalone PV/battery hybrid system is proposed that manages the power flow between the converters and the load to maintain the power balance in the system and enable the battery to support the PV array when there is a mismatch between the available PV power and the load. A multi-loop strategy is used to control the converters taking into account battery charge rate limits and state-of-charge constraints.

Unlike the tests runned in the works presented, where whenever there was a need to supply or absorb power, other units took over that role, the microgrid considered in this paper is composed of a single unit to push its limits of extreme situations as generation curtailment and load shedding regarding different load demands. So, this work adopts a grid-forming droop control strategy that has been extensively used in microgrid configurations to actively control the frequency and voltage output. Based on Guerrero et al. (2013), the strategy makes it possible to have proper power management in the microgrid unit in the face of load changes. Besides, to regulate the functioning of two DC-DC converters in the presence of operating restrictions like battery current and capacity limits, a multi-loop management method based on Mahmood et al. (2012) is implemented. This way, this paper presents a load change case study for a PV/battery unit supplying variable load demand in an islanded three-phase microgrid. Also, the operation of DC-DC converters in the presence of constraints including maximum battery current and SoC limit, performing PV curtailment when necessary. This study is essential because it demonstrates the effectiveness of the control strategies allied to manage an island microgrid unit in different extreme scenarios by analyzing the behavior of parameters such as voltages, frequency, and powers. The strategy has the following features:

- When the total load of the microgrid unit is less than PV power, the battery absorbs the surplus PV power;
- When the total load of the microgrid unit is larger than PV power, the battery provides the necessary surplus load power;
- When the total load of the microgrid unit is less than PV power and the battery is in charging current limit or SoC maximum limit, PV power curtailment is performed.

Table 1. Microgrid Parameters.

Parameter	Symbol	Value	Unit
Grid			
Nominal Voltage	E*	127	V_{rms}
Nominal Frequency	f_0	60	Hz
Nominal DC-Link Voltage	V_{dc}	300	V
DC-Link Capacitances	C_{dc}	500	μF
Filter Capacitance	C_f	18	μF
Filter Inductances	L_f, L_0	3.6, 3.6	mH
PV			
PV Power	P_{pv}	1725	W
Maximum Power Voltage	V_{mpp}	37.95	V
Maximum Power Current	I_{mpp}	9.1	A
Open Circuit Voltage	V_{oc}	46.3	V
Short Circuit Current	I_{sc}	9.6	A
BESS			
Battery Energy Capacity	E_{bat}	20	Ah
Battery Voltage	V_{bat}	205	V
SoC Limits	SoC_{lim}	20 - 90	%
Droop Control			
Droop Coeficients	m, n	0.005, 1	-
Bidirectional Buck-Boost Converter			
Bidirectional Capacitance	C_B	100	μF
Bidirectional Inductance	L_B	10	mH
2*Bidirectional Controllers	K_{pB1}, K_{iB1}	21.13, 2822.63	-
	K_{pB2}, K_{iB2}	0.042, 70	-
Boost Converter			
Boost Capacitance	C_{pv}	100	μF
Boost Inductance	L_{pv}	10	mH
4*Boost Controllers	K_{p1}, K_{i1}	$0.1257 \cdot 10^7, 0$	-
	K_{p2}, K_{i1}	0.01257, 5.341	-
	K_{pPV1}, K_{iPV1}	-0.1257, -53.41	-
	K_{pPV2}, K_{iPV2}	0.185, 3.14	-

2. MICROGRID ARCHITECTURE

The hybrid sourced microgrid analyzed in this work is illustrated in Fig. 1 and all its power and voltage characteristics are described in Table 1. The microgrid is connected to the main grid through a circuit breaker (CB), which will remain open. The unit consists of PV and BESS generation and has a three-phase grid-connection; where BESS is connected to the DC-link through a bidirectional buck-boost converter and the PV array is connected through a boost converter. The inverter is connected to the common coupling point (PCC) through an LCL filter, which helps ensure that the output impedance of the unit is mainly inductive. Load consists of three single-phase ones.

A three-phase voltage source inverter (VSI) topology is adopted for the microgrid (Barbi, 2007). The bidirectional buck-boost converter and boost converter were based in Kazimierczuk (2015). The lithium-ion battery model pre-

sented in Silva Júnior et al. (2021) was adopted to represent the BESS and it is based on the open circuit terminal voltage versus SoC relation, experimentally estimated by Baronti et al. (2013, 2014). The PV source was modeled considering equivalent circuit and mathematical functions described in Villalva et al. (2009) and MPP tracking was implemented by the perturb & observe algorithm.

3. CONTROL SYSTEMS

A grid-forming droop control structure in Fig. 1 is used to drive the VSI in islanded mode. This control comprises power calculation, droop control (Zhang et al., 2018), proportional-resonant (PR) controller (Vasquez et al., 2013), and pulse width modulation (PWM). The conventional $P - f$ and $Q - E$ droop (Zhang et al., 2018) can be applied for active and reactive power sharing, respectively. Primary droop control is responsible for giving the frequency and voltage reference and secondary droop control deals with restoring frequency and amplitude deviations (Guerrero et al., 2013, 2011). Both DC-DC converters control strategies shown in Fig. 2 use average current-mode control and were based in Mahmood et al. (2012). The pole placement technique was used to adjust the gains of the boost converter controllers, and the bidirectional buck-boost converter controllers were tunned using MATLAB/Simulink sisotool, which allows designing single-input single-output (SISO) controllers for feedback systems.

The bidirectional buck-boost converter brings more flexibility in choosing the BESS nominal voltage, allows controllable discharging, stores excess PV energy to balance the system, and supplies peak power load (Mahmood et al., 2012). This way, this converter regulates the DC-link voltage in normal operation. According to Fig. 2, bidirectional buck-boost control generates its current reference based on DC-link voltage. When BESS reaches its charging current, the i_{LB} loop controls the BESS current at $-i_{LB,min}$ due to saturation limit, enabling it to charge with constant current. Otherwise, when BESS reaches its discharge current, i_{LB} loop controls the BESS current at $i_{LB,max}$, enabling the BESS to discharge with constant current. The output of the i_{LB} loop is the PWM voltage reference responsible for controlling the switch states of the bidirectional buck-boost converter, represented by S_2 and S_3.

The boost converter is controlled to enable maximum power point tracking (MPPT) by adjusting the voltage at the PV input terminal to the maximum power point during normal operation based on system parameters including SoC, DC-link voltage, and PV maximum power. For the PV to work in MPPT, only the MPPT module produces $v_{pv,ref}$ (Fig. 2); the other two loops do not operate. Thus, the maximum power available at the PV is fed into the DC-link by the boost converter. So that the two loops cannot interfere in this situation, saturation limits were placed at the output of each PI. A positive input error signal results in an output equal to zero due to the positive saturation limit.

When BESS charges to its SoC_{max}, PV power curtailment should be performed and the boost converter starts to regulate the DC-link voltage. In order to move the PV operating point away from the maximum power point

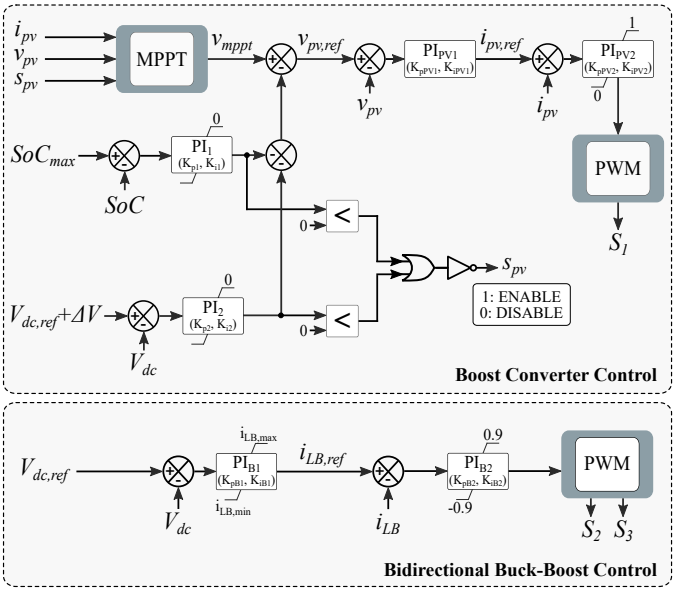

Figure 2. DC-DC converters control structure based on Mahmood et al. (2012).

(MPP), the output signal of PI_1 will be added to the MPPT voltage reference, $v_{pv,ref}$. This way, until the BESS current reaches zero and the SoC stabilizes at SoC_{max}, this loop will continue to curtail the power drawn from the PV array. PV power curtailment is performed until the balance between generation and load demand is reached. In order to disable the MPPT algorithm from keep looking for maximum power, the PI_1 output signal will be sent to a logic gate which will generate 0 in its output to disable it. From doing that, the MPPT algorithm will hold the last generated v_{mppt} value.

Also, when BESS is in charging limit, the bidirectional buck-boost converter regulates the battery current instead of the DC-link voltage. Thus, the DC-link voltage will rise as a result of the remaining energy that the battery is unable to store. In order to keep the system's power balance, the PV power must be curtailed. The DC-link voltage can be sensed by the boost converter control and can begin to be regulated once it reaches $V_{dc,ref} + \Delta V$ by using the PI_2 loop and regulating DC-link voltage at the new reference, $V_{dc,ref} + \Delta V$. Similar to how the PI_1 loop operates, the PI_2 loop begins to increase the voltage reference of the PV array whenever V_{dc} tries to increase.

4. SIMULATION RESULTS

The simulations were run in the MATLAB/Simulink environment using the parameters listed in Table 1 and the microgrid setup shown in Fig. 1. According to what was described in the control systems, the operating states of the microgrid can be divided into three scenarios: normal operation, SoC_{max} regulation and BESS current limits. To demonstrate the states, a study was conducted to show how the microgrid behaves in face of load variations. Resistive loads were defined by a constant impedance model and output power is considered to be the load power plus losses. Due to boost converter losses, PV MPPT power is regarded as 1670 W, and BESS nominal power is set to 400 W. The simulation results are described in the following

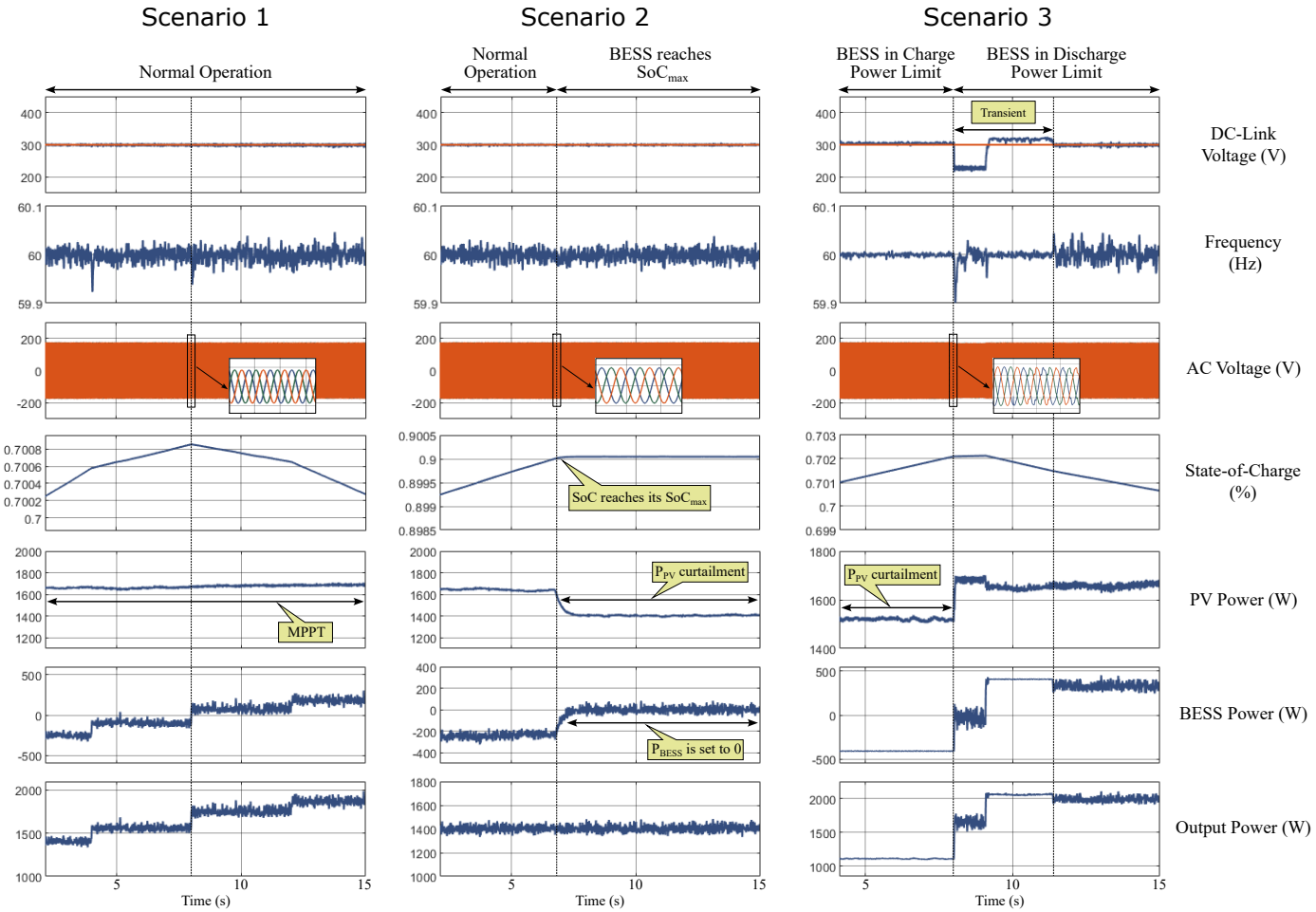

Figure 3. Simulation results.

subsections and Fig. 3 shows the DC-link voltage, output frequency, PCC voltage, state-of-charge, PV power, BESS power, load demand, and output power for all scenarios.

4.1 Scenario 1: Normal Operation

In this scenario, the load is increased step by step and the irradiance is kept constant. According to Fig. 3, while t $<$ 8 s, load power is less than PV generation and BESS charges to absorb the excess power in order to keep the DC-link voltage constant. Throughout the scenario, PV continues to work on MPPT and the bidirectional buck-boost converter regulates the DC-link voltage. In t = 8 s, load demand turns higher than PV generation and BESS discharges to compensate the imbalance between generation and load demand and also to keep the DC-link voltage constant. Toward all load changes, Fig. 3 shows that the DC-link remains stable despite the transients, AC voltage is well controlled by the PR, and frequency stays around its nominal value due to secondary droop action.

4.2 Scenario 2: BESS in Soc Maximum

In this scenario, BESS reaches its SoC maximum and the boost converter becomes responsible for regulating the DC-link voltage. Through all simulation, according to Fig. 3, the load is kept constant and its impedance is equal to $Z_L = 45\ \Omega$. When SoC reaches SoC_{max}, PI_1 loop disables the MPPT algorithm and increases the voltage reference, moving the operating point away from the MPP and reducing the boost converter current. As a result, BESS stops charging and PV exits MPPT. Meanwhile, DC-link continues to be regulated, AC voltage is well controlled by the PR, and frequency stays around its nominal value.

4.3 Scenario 3: BESS in Current Limits

Initially, load power is less than PV generation, BESS is in charging power limit and PV curtailment is performed. In this state, according to Fig. 3, $V_{dc,ref}$ is above its nominal value since PI_2 loop takes into account the sum of ΔV. In t = 8 s, load power is increased, PV power comes back to MPP and BESS starts to discharge since load demand is now higher than PV power. At this moment, BESS reaches its discharging limit and the microgrid remains stable after the transient since there is a balance between generation and load demand. If the load turns to increase again, the DC-link voltage may drop to supply the balance of the microgrid and, at this moment, load shedding should be performed. However, load shedding is considered beyond the scope of this paper. During the entire scenario, the DC-link is stable despite the transients, AC voltage is well controlled by the PR, and frequency stays around its nominal value due to secondary droop action.

5. CONCLUSIONS

This paper evaluates the power management of a hybrid photovoltaic/battery unit in an islanded microgrid. The load-interface inverter is controlled by the grid-forming droop to regulate AC voltages and frequency, while controls of boost and bidirectional buck-boost converters are controlled to meet power balance in the microgrid. The operation has been divided into three states: normal operation, maximum state-of-charge regulation, and battery current limits regulation. The transition between states is performed automatically, allowing the microgrid to operate effectively. In normal operation mode, simulation results show that the bidirectional buck-boost converter is able to regulate the DC-link voltage while the photovoltaic works in MPPT. When the battery reaches its charging limit or its maximum state-of-charge, photovoltaic generation curtailment is performed and the boost converter starts to regulate the DC-link voltage. This whole strategy enables the microgrid to work efficiently toward load changes and several battery conditions, keeping the state-of-charge within acceptable limits to increase battery useful life, allowing it to work for more cycles and thus reducing system costs related to maintenance and replacements.

ACKNOWLEDGMENT

This work was supported by the Coordination for the Improvement of Higher Education Personnel (CAPES), Brazil. The authors also want to demonstrate their thankfulness to Electrical Engineering Postgraduate Program, to Mathematics and Computational Modeling Postgraduate Program, to Informatic Center of UFPB and mainly to Digital System Laboratory (LASID) by the opportunity to develop this work.

REFERENCES

Barbi, I. (2007). *Inverter Project*. Federal University of Santa Catarina, 1 edition.

Baronti, F., Femia, N., Saletti, R., and Zamboni, W. (2014). Comparing open-circuit voltage hysteresis models for lithium-iron-phosphate batteries. In *IECON 2014 - 40th Annual Conference of the IEEE Industrial Electronics Society*, 5635–5640. doi:10.1109/IECON.2014.7049363.

Baronti, F., Zamboni, W., Femia, N., Roncella, R., and Saletti, R. (2013). Experimental analysis of open-circuit voltage hysteresis in lithium-iron-phosphate batteries. In *IECON 2013 - 39th Annual Conference of the IEEE Industrial Electronics Society*, 6728–6733. doi:10.1109/IECON.2013.6700246.

de Matos, J.G., e Silva, F.S.F., and Ribeiro, L.A.d.S. (2015). Power control in ac isolated microgrids with renewable energy sources and energy storage systems. *IEEE Transactions on Industrial Electronics*, 62(6), 3490–3498. doi:10.1109/TIE.2014.2367463.

Golsorkhi, M.S., Shafiee, Q., Lu, D.D.C., and Guerrero, J.M. (2017). A distributed control framework for integrated photovoltaic-battery-based islanded microgrids. *IEEE Transactions on Smart Grid*, 8(6), 2837–2848. doi:10.1109/TSG.2016.2593030.

Guerrero, J.M., Chandorkar, M., Lee, T.L., and Loh, P.C. (2013). Advanced control architectures for intelligent microgrids—part i: Decentralized and hierarchical control. *IEEE Transactions on Industrial Electronics*, 60(4), 1254–1262. doi:10.1109/TIE.2012.2194969.

Guerrero, J.M., Vasquez, J.C., Matas, J., de Vicuna, L.G., and Castilla, M. (2011). Hierarchical control of droop-controlled ac and dc microgrids—a general approach toward standardization. *IEEE Transactions on Industrial Electronics*, 58(1), 158–172. doi:10.1109/TIE.2010.2066534.

Karimi, Y., Oraee, H., Golsorkhi, M.S., and Guerrero, J.M. (2017a). Decentralized method for load sharing and power management in a pv/battery hybrid source islanded microgrid. *IEEE Transactions on Power Electronics*, 32(5), 3525–3535. doi:10.1109/TPEL.2016.2582837.

Karimi, Y., Oraee, H., and Guerrero, J.M. (2017b). Decentralized method for load sharing and power management in a hybrid single/three-phase-islanded microgrid consisting of hybrid source pv/battery units. *IEEE Transactions on Power Electronics*, 32(8), 6135–6144. doi:10.1109/TPEL.2016.2620258.

Kazimierczuk, M.K. (2015). *Pulse-Width Modulated DC-DC Power Converters*. Wiley, 2nd edition.

Mahmood, H. and Jiang, J. (2019). Decentralized power management of multiple pv, battery, and droop units in an islanded microgrid. *IEEE Transactions on Smart Grid*, 10(2), 1898–1906. doi:10.1109/TSG.2017.2781468.

Mahmood, H., Michaelson, D., and Jiang, J. (2012). Control strategy for a standalone pv/battery hybrid system. In *IECON 2012 - 38th Annual Conference on IEEE Industrial Electronics Society*, 3412–3418. doi:10.1109/IECON.2012.6389351.

Mahmood, H., Michaelson, D., and Jiang, J. (2015). Decentralized power management of a pv/battery hybrid unit in a droop-controlled islanded microgrid. *IEEE Transactions on Power Electronics*, 30(12), 7215–7229. doi:10.1109/TPEL.2015.2394351.

Pattabiraman, D., Lasseter, R.H., and Jahns, T.M. (2018). Comparison of grid following and grid forming control for a high inverter penetration power system. In *2018 IEEE Power Energy Society General Meeting (PESGM)*, 1–5. doi:10.1109/PESGM.2018.8586162.

Silva Júnior, G.P.d., Barros, L.S., and Barros, C.M.V. (2021). Synchronverter coupled to a lithium-ion bank for grid frequency and voltage supports and controlled charge-discharge. *Electric Power Systems Research*, 197, 107352. doi:10.1016/j.epsr.2021.107352.

Vasquez, J.C., Guerrero, J.M., Savaghebi, M., Eloy-Garcia, J., and Teodorescu, R. (2013). Modeling, analysis, and design of stationary-reference-frame droop-controlled parallel three-phase voltage source inverters. *IEEE Transactions on Industrial Electronics*, 60(4), 1271–1280. doi:10.1109/TIE.2012.2194951.

Villalva, M.G., Gazoli, J.R., and Filho, E.R. (2009). Modeling and circuit-based simulation of photovoltaic arrays. In *2009 Brazilian Power Electronics Conference*, 1244–1254. doi:10.1109/COBEP.2009.5347680.

Zhang, H., Gao, Y., and Lu, D. (2018). Micro-grid droop control strategy optimization and simulation. In *2018 China International Conference on Electricity Distribution (CICED)*, 2013–2017. doi:10.1109/CICED.2018.8592279.